# Journal of Solar Energy Research (JSER)

# Thermodynamic Analysis of Using Parabolic Trough Solar Collectors for Power and Heating Generation at the Engineering Faculty of Urmia University in Iran

M.Abdollahi Haghghi[a], S.M.Pesteei, [a*] A.chitsaz[a]

[a]Faculty of Mechanical Engineering, Urmia University, Urmia, Iran *Email: sm.pesteei@urmia.ac.ir

**ARTICLE INFO**

**A B S T R A C T**

In the present paper, the energetic and exegetic analysis of using parabolic trough solar collectors (PTSC) subsystem with an organic Rankine cycle (ORC) at the engineering faculty of Urmia University that located in Nazlou regain as a case study is carried out. The task of this cycle is to provide the heating load and electrical power of the building. Firstly the energy demand of the building is calculated. Then, by considering the geographic location and weather conditions information of Nazlou, a cycle that fits with it, in three solar radiation modes is designed. These modes are the solar mode, the solar and storage mode, and the storage mode. According to results, total heating load and electrical power rate of the building are 1253.2 kW and 1500 kW, respectively. This energy demand can be provided by 250 and 500 number of PTSC in the solar mode and the solar and storage mode, respectively. PTSC outlet temperature and its efficiency during the year are between 470-660 K and 53-56%, respectively. Heating cogeneration and electrical power energy efficiencies in the first and third mode are around 95% and 15% and in the second mode are around 45% and 7.5%, respectively. Heating cogeneration, electrical power and ORC exergy efficiencies are around 18.5%, 9.5%, and 9% in the first and third mode, respectively. For second mode these values are around 9%, 4.5%, and 4%, respectively. Also, the major exergy destruction rate is occurred in the PTSC and ORC evaporator.

## 1. Introduction

The current conditions governing to supply electrical power and heating are based on the use of fossil fuels in the most countries, and in particular in Iran. This method is an old way of converting energy into requirement energies of mankind, which generally has low efficiency, many environmental problems and a lot of costs [1,2]. Given the progress made in the field of energy conversion methods, looks like it is best to go to using the novel systems as soon as possible. Considering the very suitable solar radiation situation in Iran [3,4], one of the best ways to use novel systems is the use of solar collectors.

One of the best types of solar collectors is a parabolic trough solar collector, which has the ability to increase the fluid temperature between 60 to 400℃ with concentration ratio between 10 to 85.

PTSC is a Single-axis tracking collector, which important parts in its structure are a reflecting mirror in a parabolic shape, a receiver, and a cover that covers the receiver to reduce the heat losses [5,6]. In the following, the works that have been done about this type of collectors are mentioned.

Suman et al. [7] presented a review to increase the performance of solar collectors. Their work was focused on different aspects of the various collectors, especially PTSC.

A review in the field of design parameters, mathematical techniques and simulations used in the design of PTSCs and their applications by Hafez et al. [8] carried out. Jebasingh and Herbert [9] indicated the performance of PTSCs and reviewed the solar equipment systems such as air heating, refrigeration, industrial heating, desalination, and power systems.

The PTSC is a very good device that can be used to provide hot water for heating process [10]. Furthermore, it can be applied in power plants for electric power generation by coupling with ORC to produce superheated steam [11].

Eisavi et al. [12] analyzed a novel combined cooling, heating and power cycle with PTSCs, ORC and double effect absorption chiller. They using therminol-66, n-octane and LiBr-$H_2O$ as working fluids in the PTSC, ORC, and chiller, respectively. They concluded that energy efficiency for heating and cooling cogenerations and power production were 96%, 12.94%, and 8.9% respectively. In addition, the exergy efficiency of them were 12.8%, 4.5%, and 4.4%, respectively.

A performance evaluation of a cycle by using PTSCs for combined cooling, heating, and power production by Al-Sulaiman et al. [13] investigated. They using solar storage tank in the solar subsystem with PTSCs and using ORC and chiller equipment in three modes of solar radiations that are high, low and no radiations. Their results showed that the maximum efficiency for the low radiation times (storage did not happen) was 94%, for the high radiation times (storage happened in hot storage tank) was 47%, and for the no radiation times (using a hot storage tank) was 42%.

Marefati et al. [14] studied points of view thermal and optical of PTSC in Tehran, Tabriz, Shiraz, and Yazd which have different climate condition with the comparison between the conventional nanofluids. They indicate that Shiraz with the thermal efficiency more than 13% and annual useful energy more than 2 MW/m$^2$ is the best city for using PTSC systems.

In this paper, a case study of using PTSCs system at the engineering faculty of Urmia University, which located in Nazlou regain (in Urmia city) will be presented. This investigation by considering the various weather conditions during the year and there different solar modes of the day, proportionate with the building energy demands is carried out. The solar subsystem by coupling whit an ORC, follow two important goals that are generated electrical power and provided the heating load of the building. The next section explains how the cycle works.

## 2. System description

Present system consists of two parts that are a solar subsystem and an organic Rankine cycle (ORC). The components of the solar subsystem are parabolic trough solar collectors (PTSC), hot and cold storage tanks, a storage heat exchanger, storage pumps, a solar pump and refrigerant expansion valves. As well as, the ORC includes evaporators, a turbine, a pump, and heating process heat exchangers. There are three modes of using solar energy that are:

1. A solar mode at low solar radiations time.
2. A solar and storage mode at high solar radiations time.
3. A storage mode at night time by using thermal storage tanks.

Solar radiations by reflecting mirror of the PTSC reflect the therminol-66 oil as a working fluid, which flows inside the receiver (pipe) of the PTSC. This receiver is at the focus of the parabolic mirror.

By passing the oil from the receiver, its temperature rises. If the low solar radiations mode would have existed, just PTSC using to move the ORC part. At the high radiations time more than feeding the ORC,
PTSC by using storage tank saves solar energy to use at the night time.

Working fluid of the ORC is n-octane. This working fluid passing through the evaporator and heat exchange with therminol-66 in the form of steam enters to the turbine and then, electrical power is generated. Outlet n-octane enters the first heating process heat exchanger. Water in this heating process heated and goes to provide the engineering faculty heating load. But, it has very high energy and enters to second heating process heat exchanger. This heat exchanger using to supplies superheated vapor to laboratories, which in the building.

Then, the n-octane in the form of saturated fluid goes to ORC pump. The cycle of this paper shown in figure 1.

## 3. Modeling

In this section first, the modeling of the heat load calculations that the engineering faculty of Urmia University needed them will be presented. Also, assessment of solar energy conditions in Nazlou regain will be carried out. In addition, PTSC and thermal storage tanks, which used at the solar part of the cycle, and energetic and exegetic analysis equations of the cycle will be expressed. Heat load calculations and thermodynamic modeling of the cycle are modeled by using the carrier (HAB) and Engineering Equations Solver (EES) softwares, respectively.
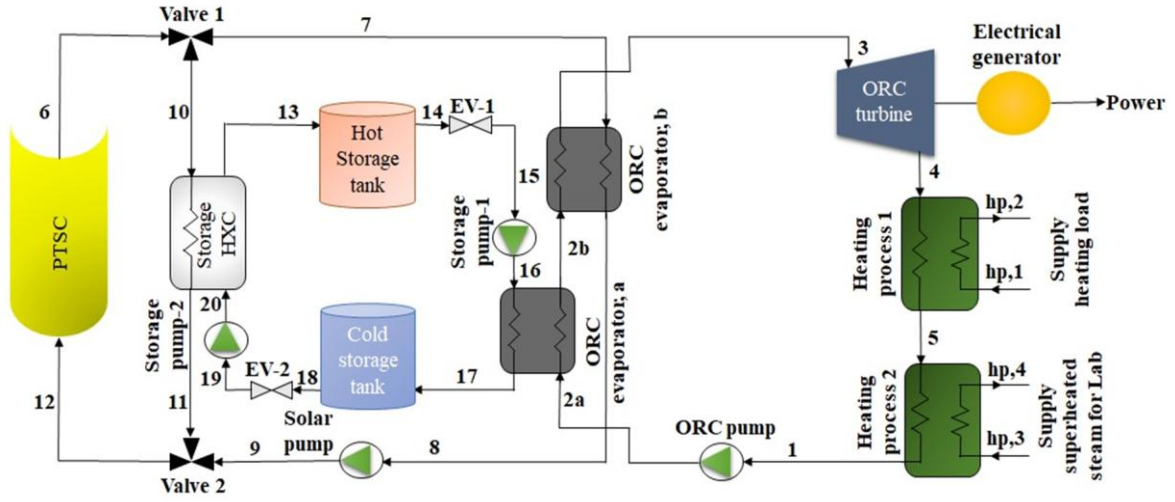
Figure 1. Schematic of the PTSC with ORC system.

### 3.1. Heat load calculations

Urmia University located at Nazlou region, which its distance from Urmia city is about 11 km. The worst ambient temperature in this place is equal to -13 °C [15]. So, heat load calculations are done based on it. The location and climate conditions of the engineering faculty of Urmia University input data listed in Table 1.

Table 1. Climate conditions and geographical location information of Nazlou regain.

| Latitude | 37.7 (Deg) |
|---|---|
| Longitude | -45.0 (Deg) |
| Elevation | 1363.0 (m) |
| Winter Design Dry-Bulb | -12.0 (°C) |
| Winter Design Wet-Bulb | -13.0 (°C) |
| Winter Design Wet-Bulb | 1.00 |
| Average Ground Reflectance | 1.385 (W/(m-K)) |

Heat load rate of a place obtained through calculations of three types of heating process, which are 1.Heat transfer of any component of location, 2.Air ventilation and 3. Heat load rate of hot water consumed. Carrier software calculated first and second process. So, hot water consumed heating load rate [16] can be defined as

$$\dot{Q}_{h,c} = 8.33.[\,j.(\Sigma y_i.N_i)].\Delta T_{h,c} \qquad (1)$$

where $\Delta T_{h,c}$ is the temperature difference between hot water consumed and town water which are 140 °F and 60 °F, respectively, j is the demand factor, $y_i$ is the maximum hot water consumed rate of each place that needed it, and N is the number of each place that needed hot water.

So, the total heat loads rate [16] expressed as

$$\dot{Q}_{tot} = \dot{Q}_{H} + \dot{Q}_{h,c} \qquad (2)$$

where $\dot{Q}_{H}$ is the heat losses rate.

### 3.2. Performance analysis

In this section by presentation received solar energy in Nazlou regain, performance analysis of using PTSC carried out.

### 3.2.1. Solar energy in Nazlou

The most important parameters that should be defined is the beam radiation on a horizontal surface rate. So, the under steps are followed to obtain this value. The solar altitude angle [5,6] is

$$\sin(\alpha) = \cos(\varphi).\cos(\omega).\cos(\delta) + \sin(\varphi).\sin(\delta) \qquad (3)$$

where $\varphi$ is the latitude angle, $\omega$ is the solar hour angle, $\delta$ is the solar declination angle.

$$\delta = 23.46 \sin(\frac{360.(N+284)}{365}) \qquad (4)$$

$$\omega = 15.(t-12) \qquad 1 \le t \le 24 \qquad (5)$$

$Z_s$ is the solar azimuth angle [5,6] and can be presented as

$$\sin(Z_s) = \frac{\cos(\delta).\sin(\omega)}{\cos(\alpha)} \qquad (6)$$

where N is the day number and t is the time.

Monthly average daily total insolation on an extraterrestrial horizontal surface [17] can be defined as

$$\bar{H}_0 = \frac{24 \times 3600}{\pi}.I_{sc}.[1+0.033.\cos(\frac{360\,N}{365})]$$
$$.[\cos(\varphi).\sin(\omega_s).\cos(\delta) \qquad (7)$$
$$+ \frac{\pi\omega_s}{180}.\sin(\varphi).\sin(\delta)]$$

where $I_{sc}$ is the solar constant that is 1353 W/m$^2$.

As well as, monthly average daily insolation on a terrestrial horizontal surface equation [18] is as follows

$$\bar{H} = \bar{K}_t.\bar{H}_0 \qquad (8)$$

where $\bar{K}_t$ is the monthly average clearness index, $\omega_s$ is the hour angle at sunrise or sunset can be written as

$$\omega_s = \cos^{-1}(-\tan(\varphi).\tan(\delta)) \qquad (9)$$

Now, by calculating the monthly average daily diffuse radiation on a horizontal surface ($\bar{H}_d$) from the following equation, the monthly average daily beam radiation on a horizontal surface ($\bar{H}_b$) can be defined [5,6].

$$\frac{\overline{H}_d}{\overline{H}} = 1.390 - 4.027.\overline{K}_t + 5.531.\overline{K}_t^2 + 3.108.\overline{K}_t^3 \qquad (10a)$$

$$\overline{H}_b = \overline{H} - \overline{H}_d \qquad (10b)$$

Finally, beam radiation on a horizontal surface rate [5,6] is

$$G_b = \frac{\overline{H}_b}{t} \qquad (11)$$

### 3.2.2. Modeling of parabolic trough solar collectors

By considering to above calculations, in this section the modeling of the PTSC is presented. The input data used in the cycle analysis is given in Table 2.

The absorbed solar radiation rate by the PTSC receiver [19] is as follows

$$S = G_b.\eta_r \qquad (12)$$

where $\eta_r$ is the receiver efficiency [5,6] that calculated from

$$\eta_r = \rho_c.\gamma.\tau.\alpha.k_\gamma \qquad (13)$$

where $\rho_c$ is the reflectance coefficient of the mirror, $\gamma$ is the intercept factor, $\tau$ is the transmittance of the glass cover, $\alpha$ is the absorbance of the receiver, and $k_\gamma$ is the incidence angle modifier.

The useful power from the PTSC [5,6] can be expressed as

$$\dot{Q}_u = A_{ap}.F_R.(S - \frac{A_r}{A_{ap}}.U_L.(T_{r,i} - T_0) \qquad (14)$$

where $A_{ap}$ is the PTSC aperture area, $F_R$ is the heat removal factor, $A_r$ is the PTSC receiver area, $U_L$ is the PTSC overall heat loss coefficient. $T_{r,i}$ and $T_0$ are temperatures of the receiver inlet and ambient, respectively.

By using following equations the aperture area of the PTSC and receiver area [5,6] can be obtained.

$$A_{ap} = (w - D_{c,o}).L \qquad (15a)$$

$$A_r = \pi.D_{r,o}.L \qquad (15b)$$

where w is the width of the PTSC, $D_{c,o}$ and $D_{r,o}$ are the outlet diameter of the cover and receiver, respectively, and L is the length of the PTSC.

The heat removal factor [5,6] calculated by

$$F_R = \frac{\dot{m}_r.C_{pr}}{A_r.U_L}.[1 - \exp(-\frac{A_r.U_L.F_1}{\dot{m}_r.C_{pr}})] \qquad (16)$$

where $C_{pr}$ is the oil specific heat in the PTSC receiver and $F_1$ is the PTSC efficiency factor [5,6] and written as

$$F_1 = \frac{U_o}{U_L} \qquad (17)$$

The heat loss coefficient between the ambient and receiver of the PTSC depends on three types of heat transfer coefficients, which are 1.The convection heat transfer coefficient between the cover and the ambient ($h_{c,ca}$), 2.The radiation heat transfer coefficient between the cover and ambient ($h_{r,ca}$), and 3.The radiation heat transfer coefficient between the cover and receiver ($h_{r,cr}$). So, overall heat loss coefficient [14] defined as

$$U_L = [\frac{A_r}{(h_{c,ca} + h_{r,ca}).A_c} + \frac{1}{h_{r,cr}}]^{-1} \qquad (18)$$

where $A_c$ is the cover area of the PTSC [14]. This value can be expressed as

$$A_c = \pi.D_{c,o}.L \qquad (19)$$

The convection heat transfer coefficient between the cover and the ambient [14] is as follows

$$h_{c,ca} = \frac{Nus.k_{air}}{D_{c,o}} \qquad (20)$$

where Nus is the Nusselt number and $k_{air}$ is the thermal conductivity of the air.

The radiation heat coefficient between the cover and ambient is [14] defined as

$$h_{r,ca} = [\varepsilon_{cv}.\sigma.(T_c + T_a).(T_c^2 + T_a^2)] \qquad (21)$$

where $T_c$ and $T_a$ are the temperatures of the cover and ambient, respectively, $\varepsilon_{cv}$ is the emittance, and $\sigma$ is the Stefane Boltzmann constant.

Finally, the radiation heat transfer coefficient between the cover and receiver [14] obtained by

$$h_{r,cr} = \frac{\sigma.(T_c + T_{r,av}).(T_c^2 + T_{r,av}^2)}{\frac{1}{\varepsilon_r} + \frac{A_r}{A_c}.(\frac{1}{\varepsilon_{cv}} - 1)} \qquad (22)$$

The overall heat transfer coefficient of the PTSC [14] can be written as

$$U_O = [\frac{1}{U_L} + \frac{D_{r,o}}{h_{c,r,in}.D_{r,i}} + (\frac{D_{r,o}}{2.K_r}.\ln(\frac{D_{r,o}}{D_{r,i}}))]^{-1} \qquad (23)$$

where $h_{c,r,in}$ is the convective heat transfer coefficient inside the receiver pipe [14], which defined as

$$h_{c,r,in} = \frac{Nus_r.k_r}{D_{r,i}} \qquad (24)$$

The cover average temperature [14] can be obtained from

$$T_c = \frac{h_{r,cr}.T_{r,av} + \frac{A_c}{A_r}.(h_{c,ca} + h_{r,ca}).T_0}{h_{r,cr} + \frac{A_c}{A_r}.(h_{c,ca} + h_{r,ca})} \qquad (25)$$

PTSC outlet temperature [5,6] calculated by

$$T_{PTSC,O} = T_{PTSC,i} + \frac{\dot{Q}_u}{\dot{m}_r.C_{p,r}} \qquad (26)$$

And its efficiency [5,6] can be defined as

$$\eta_{PTSC} = F_R.[\eta_r - U_L.(\frac{T_{PTC,i} - T_0}{G_b(A_{ap}/A_r)})] \times 100 \qquad (27)$$

### 3.2.3. Storage tanks

The simulation of the storage tanks based on charging, storing, and discharging, by using the oil can be presented as

| a) Parameter | b) Value | c) Reference |
|---|---|---|
| d) ORC | | |
| e) ORC turbine efficiency | f) 80% | g) [13] |
| h) ORC pump efficiency | i) 80% | j) [13] |
| k) Effectiveness of the ORC evaporator | l) 85% | m) [13] |
| n) PTSC | | |
| o) PTSC width | p) 5.76 m | q) [13] |
| r) PTSC lenght | s) 12.27 m | t) [13] |
| u) Inlet diameter of receiver | v) 0.066 | w) [5] |
| x) Outlet diameter of receiver | y) 0.07 | z) [5] |
| aa) Inlet diameter of cover | bb) 0.0109 | cc) [5] |
| dd) Outlet diameter of cover | ee) 0.115 | ff) [5] |
| gg) Reflectance factor of the mirror | hh) 0.931 | ii) [5] |
| jj) Intercept factor | kk) 0.93 | ll) [5] |
| mm) Transmittance of the glass cover | nn) 0.94 | oo) [5] |
| pp) Absorbance of the receiver | qq) 0.94 | rr) [5] |
| ss) Incidence angle modifier | tt) 1 | uu) [5] |
| vv) Stefane-Boltzmann constant | ww) 5.76 *10⁻⁸ kW/m².K⁴ | xx) [5] |
| yy) Emittance of the receiver | zz) 0.92 | aaa) [5] |
| bbb) Emittance of the receiver cover | ccc) 0.87 | ddd) [5] |
| eee) Mass flow rate in the receiver | fff) 0.35 kg/s | ggg) [5] |

Table 2. Input data of the cycle.

*3.2.3.1. Hot storage tank in charging time*

The heat rate enters the hot storage tank [13] is as follows

$$\dot{Q}_{hst} = \dot{Q}_{13} - \dot{Q}_{l,hst} \tag{28}$$

Subscripts hst and l,hst explains the hot storage tank and the lost heat from the hot storage tank, respectively.

The lost heat from the hot storage tank [13] can be calculated by using

$$\dot{Q}_{l,hst} = U.A_h.(T_{hst} - T_0) \tag{29}$$

where U is the overall heat transfer coefficient of the storage tank.

The total heat achieved by the hot storage tank [13] is defined as

$$\Sigma Q_{hst} = \dot{Q}_{hst}.\Delta t_h \tag{30}$$

where $\Delta t_h$ is the total time of charging in the hot storage tank.

By considering that $M_{hst}$ is the total mass of the oil in the hot storage tank, the temperature in the storage tank [13] is

$$T_{hst} = \frac{\Sigma Q_{hst}}{C_{p,hst}.M_{hst}} \tag{31}$$

*3.2.3.2. Hot storage tank in storing time*

The temperature of the oil in the tank changes with time [13]. So, this value can be written as

$$T_{hst}^+ = T_{hst} + \frac{\Delta t_h}{C_{p,hst}.M_{hst}}.(-UA_h.(T_{hst} - T_0)) \tag{32}$$

The total heat loss of the oil during storing time in the hot storage tank [13] is

$$Q_{hst,tlost} = C_{p,hst}.M_{hst}.(T_{hst} - T_{hst}^+) \tag{33}$$

*3.2.3.3. Hot storage tank in discharging time*

The amount of the total heat at discharging time in hot storage tank [13] can be expressed as

$$Q_{14} = \Sigma Q_{hst} - Q_{hst,tlost} \qquad (34)$$

### 3.2.3.4. Cold storage tank in storing time

The total heat in the cold storage tank at storing time [13] is

$$Q_{cst,tlost} = C_{p,cst}.M_{cst}.(T_{cst} - T_{cst}^+) \qquad (35)$$

where Subscript cst show the cold storage tank.

The temperature of the oil in the cold storage tank [13] expressed as

$$T_{cst}^+ = T_{cst} + \frac{\Delta t_c}{C_{p,cst}.M_{cst}}.(-UA_c.(T_{cst} - T_0)) \qquad (36)$$

### 3.2.3.5. Cold storage tank in discharging time

The total amount of the heat at discharging time from the oil in the cold storage tank [13] is

$$Q_{18} = \Sigma Q_{cst} - Q_{cst,tlost} \qquad (37)$$

### 3.3. Energetic and exegetic analysis

First low of thermodynamic for each component by neglecting kinetic and potential energy [20,21] can be written as

$$\dot{Q} - \dot{W} = \Sigma \dot{m}_e.h_e - \Sigma \dot{m}_i.h_i \qquad (38)$$

where $\dot{Q}$, $\dot{W}$, $\dot{m}$ and h are the heat transfer rate and work transfer rate, mass flow rate, and specific enthalpy, respectively.

Exergy described as the maximum potential rate of the work that given through the process [20,21]. So, this analysis for each component by neglecting kinetic and potential exergy [20,21] is

$$\dot{I} = \Sigma(1 - \frac{T_0}{T_j})\dot{Q}_j - \dot{W}_{cv} + \sum \dot{EX}_i - \sum \dot{EX}_e \qquad (39a)$$

$$\sum \dot{EX} = \dot{m}.[(h - h_0) - T_0.(s - s_0)] \qquad (39b)$$

where $\dot{I}$ and $\dot{EX}$ are exergy destruction rate and exergy rate, respectively.

These two analysis are given in Table 3 for each component of the cycle.

### 3.4. Overall performance analysis of the cycle

The net electrical power of the cycle [12] is as follows

$$\dot{W}_{net} = \eta_g.\dot{W}_{oT} - \dot{W}_{oP}/\eta_m - \dot{W}_{sol,P}/\eta_m \\ -\dot{W}_{st1,P}/\eta_m - \dot{W}_{st2,P}/\eta_m \qquad (40)$$

The net electrical power energy and exergy efficiencies [12] obtained from

$$\eta_{en,elec} = \frac{\dot{W}_{net}}{\dot{Q}_{in}} \qquad (41a)$$

$$\eta_{ex,elec} = \frac{\dot{W}_{net}}{\dot{EX}_{\dot{Q}_{in}}} \qquad (41b)$$

The energy and exergy efficiencies of the heating cogeneration [12] can be expressed as

$$\eta_{en,cog,H} = \frac{\dot{W}_{net} + \dot{Q}_H}{\dot{Q}_{in}} \qquad (42a)$$

$$\eta_{ex,cog,H} = \frac{\dot{W}_{net} + \dot{m}_{hp}.(ex_{hp,1} - ex_{hp,2})}{\dot{EX}_{\dot{Q}_{in}}} \qquad (42b)$$

where $\dot{EX}_{\dot{Q}_{in}}$ denotes the exergy rate input to the PTSC or storage tank, which in reference 22 fully explained.

## 4. Results and discussions

In this section, the energy demand calculations results of the engineering faculty of Urmia University are discussed. Also, thermodynamic analysis results based on energetic and exegetic modeling of the solar system with organic Rankine cycle are expressed. The building heat load and its electrical power demand are given in Table 4. Thermodynamic properties of each point in this study for three modes in the cycle are shown in Tables 5-7. The thermodynamic assessment of the cycle based on four parameters, which are the day number of the year, ORC pump inlet temperature, ORC turbine inlet pressure, and PTC outlet temperature are examined. Finally, the exergy destruction rate for each component is presented.

### 4.1. Energy demand calculations results

The engineering faculty of Urmia University consists of five floors. The total area of this building is more than 9800 m². According to the research, its maximum electrical power rate is about 1500 kW. Achieved heating loads results for each floor are listed in Table 4. The total heating load is 1253.2 kW. So, by considering 20% safety factor the first heating process heat exchanger should supply 1504 kW. Second heating process heat exchanger supplies superheated water for laboratories, which are in the building.

### 4.2. Thermodynamic analysis results

In three different solar radiation modes, which are only solar mode, solar and storage mode, and storage mode this cycle analyzed. Tables 5-7 show the thermodynamic properties of each point at the cycle for three mentioned modes, respectively. These tables are presented based on temperature, pressure, vapor pressure, mass flow rate, specific enthalpy, and specific exergy.

### 4.2.1. Effects of the days

The influences of the days in the year on the cycle operation are shown in figures 2-4. In figure 2, the monthly average solar radiation on a horizontal surface and the monthly average daily absorbed solar radiation rate by the PTSC receiver in Nazlou regain climate conditions are plotted.

| Table 3. Energy rate and exergy rate balance of each component [20]. | | |
|---|---|---|
| Component | Energy rate balance | Exergy rate balance |
| PTSC in the solar mode | $\dot{Q}_{PTSC} = \dot{m}_{sol}.(h_6 - h_{12})$ | $\dot{EX}_{d,PTSC} = (\dot{EX}_{12} - \dot{EX}_6 + \dot{EX}_{PTSC}).\Delta t_{h,solar} / 24[hr]$ |
| PTSC in the solar and storage mode | $\dot{Q}_{PTSC} = \dot{m}_{sol,st}.(h_6 - h_{12})$ | $\dot{EX}_{d,PTSC} = (\dot{EX}_{12} - \dot{EX}_6 + \dot{EX}_{PTSC}).\Delta t_{hdhst} / 24[hr]$ |
| HST in the solar and storage mode | $\dot{m}_{13}.h_{13} - \dot{Q}_{l,hst} = \dot{Q}_{hst}$ | $\dot{EX}_{d,HST} = (\dot{EX}_{13} - \dot{EX}_{14}).\Delta t_{hdcst} / 24[hr]$ |
| HST in the storage mode | $\dot{m}_{14}.h_{14} - \dot{Q}_{hst} = \dot{Q}_{hst,tlost}$ | $\dot{EX}_{d,HST} = (\dot{EX}_{13} - \dot{EX}_{14}).\Delta t_{hchst} / 24[hr]$ |
| CST in the solar and storage mode | $\dot{m}_{17}.h_{17} - \dot{Q}_{l,cst} = \dot{Q}_{cst}$ | $\dot{EX}_{d,CST} = (\dot{EX}_{17} - \dot{EX}_{18}).\Delta t_{hdhst} / 24[hr]$ |
| CST in the storage mode | $\dot{m}_{18}.h_{18} - \dot{Q}_{cst} = \dot{Q}_{cst,tlost}$ | $\dot{EX}_{d,CST} = (\dot{EX}_{17} - \dot{EX}_{18}).\Delta t_{hchst} / 24[hr]$ |
| Storage HXC | $\dot{m}_{11}.h_{11} - \dot{m}_{10}.h_{10} = \dot{m}_{13}.h_{13} - \dot{m}_{20}.h_{20}$ | $\dot{EX}_{d,SHXC} = (\dot{EX}_{10} - \dot{EX}_{11} + \dot{EX}_{20} - \dot{EX}_{13}).\Delta t_{h,solar} / 24[hr]$ |
| Storage pump-1 | $\dot{W}_{sp1} = \dot{m}_{16}.h_{16} - \dot{m}_{15}.h_{15}$ | $\dot{EX}_{d,sp1} = (\dot{EX}_{15} - \dot{EX}_{16} + \dot{W}_{sp1}).\Delta t_{hdhst} / 24[hr]$ |
| Storage pump-2 | $\dot{W}_{sp2} = \dot{m}_{20}.h_{20} - \dot{m}_{19}.h_{19}$ | $\dot{EX}_{d,sp2} = (\dot{EX}_{19} - \dot{EX}_{20} + \dot{W}_{sp2}).\Delta t_{hchst} / 24[hr]$ |
| Solar pump | $\dot{W}_{sol,p} = \dot{m}_9.h_9 - \dot{m}_8.h_8$ | $\dot{EX}_{d,sol,p} = (\dot{EX}_8 - \dot{EX}_9 + \dot{W}_{sol,p}).\Delta t_{h,solar} / 24[hr]$ |
| EV-1 | $\dot{m}_{14}.h_{14} = \dot{m}_{15}.h_{15}$ | $\dot{EX}_{d,EV-1} = (\dot{EX}_{15} - \dot{EX}_{14}).\Delta t_{hdhst} / 24[hr]$ |
| EV-2 | $\dot{m}_{18}.h_{18} = \dot{m}_{19}.h_{19}$ | $\dot{EX}_{d,EV-2} = (\dot{EX}_{18} - \dot{EX}_{19}).\Delta t_{hchst} / 24[hr]$ |
| ORC evaporator-a | $\dot{m}_{17}.h_{17} - \dot{m}_{16}.h_{16} = \dot{m}_3.h_3 - \dot{m}_{2a}.h_{2a}$ | $\dot{EX}_{d,ev-a} = (\dot{EX}_{16} - \dot{EX}_{17} + \dot{EX}_{2a} - \dot{EX}_3).\Delta t_{hdhst} / 24[hr]$ |
| ORC evaporator-b | $\dot{m}_8.h_8 - \dot{m}_7.h_7 = \dot{m}_3.h_3 - \dot{m}_{2b}.h_{2b}$ | $\dot{EX}_{d,ev-b} = (\dot{EX}_7 - \dot{EX}_8 + \dot{EX}_{2b} - \dot{EX}_3).(24 - \Delta t_{hdhst}) / 24[hr]$ |
| ORC turbine | $\dot{W}_T = \dot{m}_3.h_3 - \dot{m}_4.h_4$ | $\dot{EX}_{d,T} = \dot{EX}_3 - \dot{EX}_4 - \dot{W}_T$ |
| ORC heating process 1 | $\dot{m}_5.h_5 - \dot{m}_4.h_4 = \dot{m}_{hp,2}.h_{hp,2} - \dot{m}_{hp,1}.h_{hp,1}$ | $\dot{EX}_{d,HP1} = \dot{EX}_3 - \dot{EX}_4 + \dot{EX}_{hp,1} - \dot{EX}_{hp,2}$ |
| ORC heating process 2 | $\dot{m}_1.h_1 - \dot{m}_5.h_5 = \dot{m}_{hp,4}.h_{hp,4} - \dot{m}_{hp,3}.h_{hp,3}$ | $\dot{EX}_{d,HP2} = \dot{EX}_4 - \dot{EX}_5 + \dot{EX}_{hp,3} - \dot{EX}_{hp,4}$ |
| ORC pump | $\dot{W}_{op} = \dot{m}_2.h_2 - \dot{m}_1.h_1$ | $\dot{EX}_{d,op} = \dot{EX}_1 - \dot{EX}_2 + \dot{W}_{op}$ |

The monthly average daily total radiation on a horizontal surface varies 7 to 25 MJ/m$^2$ per a day during the year. As well as, monthly average daily beam solar radiation on a horizontal surface is between 4 to 17 MJ/m$^2$ per a day.

| Table 4. Heating load calculations relates. | | |
|---|---|---|
| Zone Name | Heating Load (kW) | Floor Area (m²) |
| Ground floor | 578.7 | 5910.9 |
| First floor | 249.6 | 2105.2 |
| Second floor | 84.2 | 850.9 |
| Third floor | 55.9 | 488.7 |
| Fourth floor | 56.3 | 448.3 |
| Hot water consumed | 228.5 | ____ |
| Total | 1253.2 | 9804 |

The PTSC outlet temperature and its efficiency based on different days of the year are presented in figure 3. The minimum outlet temperature is 470 K, in this mode, the efficiency is equal to 53.5%.
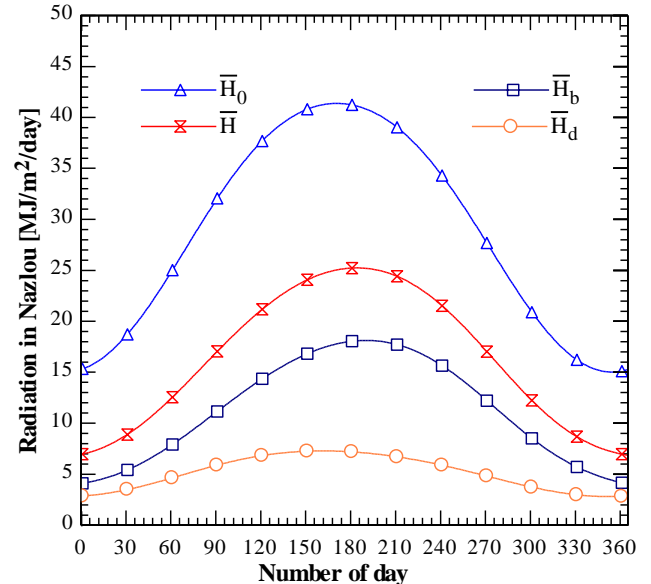


Figure 2. Monthly average daily solar radiation on a horizontal surface in Nazlou during the year.
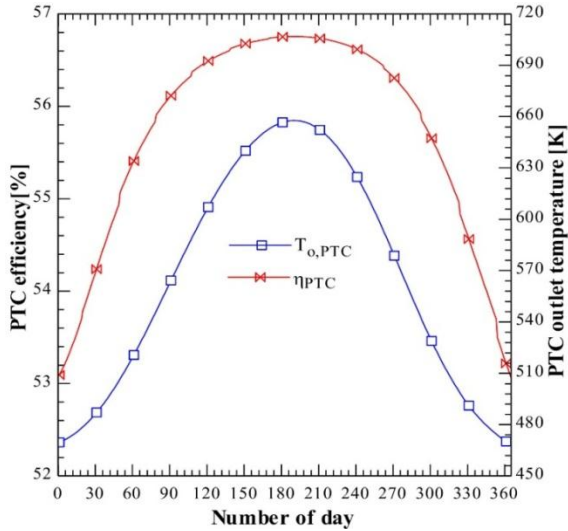
Figure 3. Outlet temperature from the PTSC and its efficiency during the year.

While the most outlet temperate is 660 K at the summer days. Corresponding to this mode the efficiency is more than 56% in Nazlou regain.

Figure 4 shows the numbers of the PTSC and their total aperture area that needed to supply energy demand of the building in the solar mode and the solar and storage mode.

In the solar and storage mode, the most numbers of the PTSC in the winter days are 1601 that their total aperture areas are 110264 m$^2$. Also, in the solar mode 952 and 65685 m$^2$ are the maximum values of these parameters, respectively.

### 4.2.2. Effects of the ORC pump inlet temperature

The effects of the ORC pump inlet temperature of the cycle performance from points of view energy and exergy efficiencies are given in figures 5 and 6 in the three solar radiation modes.
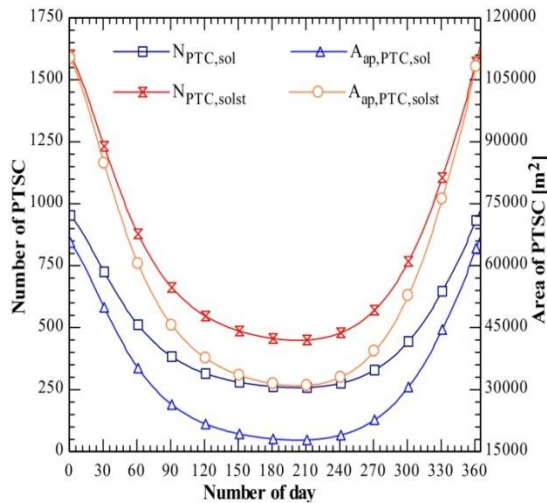


Figure 4. The numbers of the PTSC and their total aperture area in the solar mode and the solar and storage mode.

In figure 5, by increasing temperature heating cogeneration energy efficiency is increased. But electrical power energy efficiency is decreased. As seen in the figure the solar mode and the storage mode efficiencies are equal together. This result is due to the fact that the amount of energy that these two states give to the ORC are equals. Because the ORC part is bound to supply energy. So, this state exists in all analyses. In the solar mode and the storage mode the efficiencies are more than the solar and storage mode. In the solar mode and the storage mode, heating cogeneration efficiency and electrical efficiency are around 95% and 15.5%, respectively. In the solar and storage mode, these values are around 45% and 7.5%, respectively.

The heating cogeneration, electrical power, and ORC exergy efficiencies based on ORC pump inlet temperature for three solar radiation modes are plloted in figure 6. It can be seen that the exergy efficiencies with ORC pump outlet temperature have an inverse relationship with a little slope. In the solar mode and the storage mode heating cogeneration, electrical power, and ORC exergy efficiencies are around 18.5%, 9.5%, and 9%, respectively. For the solar and storage mode, these values are 9%, 4.5%, and 4%, respectively.
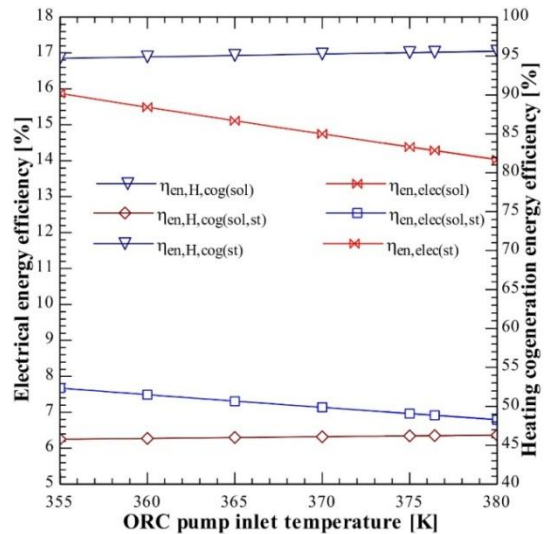


Figure 5. Effect of the ORC pump inlet temperature on the energy efficiencies.

### 4.2.3. Effects of the turbine inlet pressure

In figures 7 and 8 based on turbine inlet pressure, energy and exergy efficiencies of the cycle are drawn. Firstly, the effects of the turbine inlet pressure on the heating cogeneration and electrical power energy efficiencies are presented in figure 7. It is observed that in each solar radiation modes by increasing inlet pressure of the turbine both mentioned values are increased.

| State no. | Fluid | T [K] | P [kPa] | Pv [kPa][a] | ṁ [kg/s] | h [kJ/kg] | e [kJ/kg] |
|---|---|---|---|---|---|---|---|
| 1 | n-octane | 365 | 35.8 | | 15.21 | 157.5 | 15.58 |
| 2 | n-octane | 365.9 | 2000 | | 15.21 | 161.3 | 18.77 |
| 3 | n-octane | 553 | 2000 | | 15.21 | 840.5 | 270.1 |
| 4 | n-octane | 480.5 | 35.8 | | 15.21 | 736.7 | 150 |
| 5 | n-octane | 438.5 | 35.8 | | 15.21 | 637.8 | 115.3 |
| 6 | Therminol-66 | 600 | | 54.05 | 12.5 | 1602 | 704.9 |
| 7 | Therminol-66 | 600 | | 54.05 | 12.5 | 1602 | 704.9 |
| 8 | Therminol-66 | 401 | | 0.1671 | 12.5 | 775.2 | 151.5 |
| 9 | Therminol-66 | 401 | | 0.1671 | 12.5 | 775.2 | 151.5 |
| 12 | Therminol-66 | 401 | | 0.1671 | 12.5 | 835.7 | 186.9 |
| hp,1 | Water | 303.2 | 101.3 | | 8.9 | 167.6 | 1.527 |
| hp,2 | Water | 343.2 | 101.3 | | 8.9 | 335 | 18.94 |
| hp,3 | Water | 298.2 | 101.3 | | 2.6 | 104.8 | 0 |
| hp,4 | Water | 473.2 | 101.3 | | 2.6 | 2875 | 545.6 |

Table 5. Thermodynamic properties for the solar mode.

[a] EES software just can be calculated the vapor pressure for therminol-66.

| State no. | Fluid | T [K] | P [kPa] | Pv [kPa][a] | ṁ [kg/s] | h [kJ/kg] | e [kJ/kg] |
|---|---|---|---|---|---|---|---|
| 1 | n-octane | 365 | 35.8 | | 15.21 | 157.5 | 15.58 |
| 2 | n-octane | 365.9 | 2000 | | 15.21 | 161.3 | 18.77 |
| 3 | n-octane | 553 | 2000 | | 15.21 | 840.5 | 270.1 |
| 4 | n-octane | 480.5 | 35.8 | | 15.21 | 736.7 | 150 |
| 5 | n-octane | 438.5 | 35.8 | | 15.21 | 637.8 | 115.3 |
| 6 | Therminol-66 | 600 | | 54.05 | 27.88 | 1602 | 704.9 |
| 7 | Therminol-66 | 600 | | 54.05 | 12.5 | 1602 | 704.9 |
| 8 | Therminol-66 | 401 | | 0.1671 | 12.5 | 775.2 | 151.5 |
| 9 | Therminol-66 | 401 | | 0.1671 | 12.5 | 775.2 | 151.5 |
| 10 | Therminol-66 | 600 | | 54.05 | 15.38 | 1602 | 704.9 |
| 11 | Therminol-66 | 432.3 | | 0.5644 | 15.38 | 884.8 | 216.5 |
| 12 | Therminol-66 | 418.5 | | 0.3371 | 27.88 | 835.7 | 186.9 |
| 13 | Therminol-66 | 558.1 | | 22.09 | 16.67 | 1401 | 560.2 |
| 18 | Therminol-66 | 390.4 | | 16.67 | 16.67 | 739.5 | 131.1 |
| 19 | Therminol-66 | 390.4 | | 16.67 | 16.67 | 739.5 | 131.1 |
| 20 | Therminol-66 | 390.4 | | 16.67 | 16.67 | 739.5 | 131.1 |
| hp,1 | Water | 303.2 | 101.3 | | 8.9 | 167.6 | 1.527 |
| hp,2 | Water | 343.2 | 101.3 | | 8.9 | 335 | 18.94 |
| hp,3 | Water | 298.2 | 101.3 | | 2.6 | 104.8 | 0 |
| hp,4 | Water | 473.2 | 101.3 | | 2.6 | 2875 | 545.6 |

Table 6. Thermodynamic properties for the solar and storage mode.

[a] EES software just can be calculated the vapor pressure for therminol-66.

| Table 7. Thermodynamic properties for the storage mode. | | | | | | | |
|---|---|---|---|---|---|---|---|
| State no. | Fluid | T [K] | P [kPa] | Pv [kPa][a] | ṁ [kg/s] | h [kJ/kg] | e [kJ/kg] |
| 1 | n-octane | 365 | 35.8 | | 15.21 | 157.5 | 15.58 |
| 2 | n-octane | 365.9 | 2000 | | 15.21 | 161.3 | 18.77 |
| 3 | n-octane | 553 | 2000 | | 15.21 | 840.5 | 270.1 |
| 4 | n-octane | 480.5 | 35.8 | | 15.21 | 736.7 | 150 |
| 5 | n-octane | 438.5 | 35.8 | | 15.21 | 637.8 | 115.3 |
| 14 | Therminol-66 | 551.3 | | 18.8 | 16.67 | 1370 | 538.5 |
| 15 | Therminol-66 | 551.3 | | 18.8 | 16.67 | 1370 | 538.5 |
| 16 | Therminol-66 | 551.3 | | 18.8 | 16.67 | 1370 | 538.5 |
| 17 | Therminol-66 | 393.7 | | 0.1237 | 16.67 | 750.6 | 177.9 |
| hp,1 | Water | 303.2 | 101.3 | | 8.9 | 167.6 | 1.527 |
| hp,2 | Water | 343.2 | 101.3 | | 8.9 | 335 | 18.94 |
| hp,3 | Water | 298.2 | 101.3 | | 2.6 | 104.8 | 0 |
| hp,4 | Water | 473.2 | 101.3 | | 2.6 | 2875 | 545.6 |
| [a] EES software just can be calculated the vapor pressure for therminol-66. | | | | | | | |
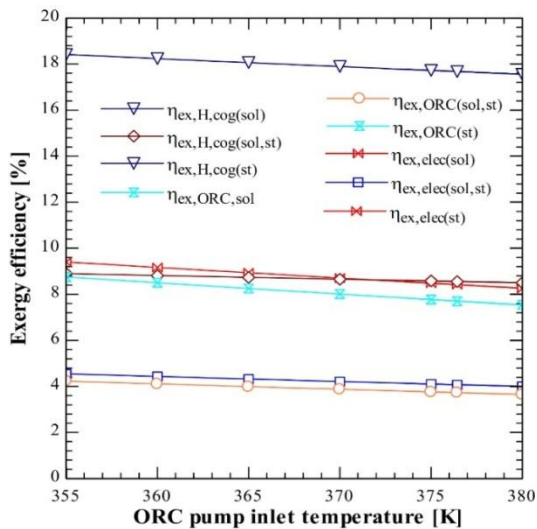


Figure 6. Effect of the ORC pump inlet temperature on the exergy efficiencies.
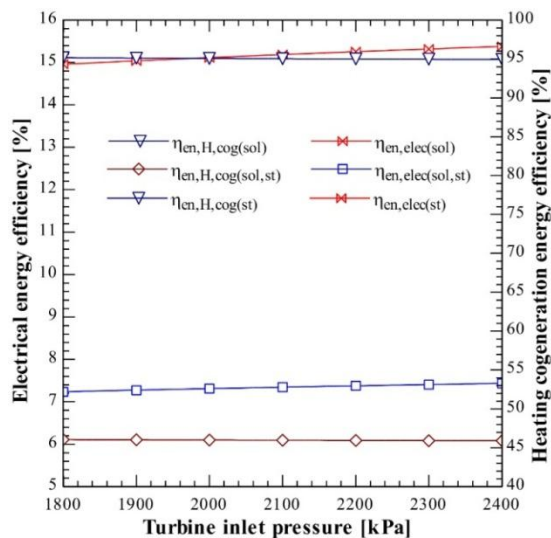


Figure 7. Effect of the turbine inlet pressure on the energy efficiencies.

Figure 8 indicate the effects of the turbine inlet pressure on the heating cogeneration, electrical power, and ORC exergy efficiencies. Unlike ORC pump inlet temperature influence, here, by increasing pressure, the exergy efficiencies are increased.

### 4.2.4. Effects of the PTSC outlet temperature

The PTSC outlet temperature is the most important parameter in this cycle. Because, based on it, present system is worked. The effects of this parameter are shown in figure 9-11. In figure 9 the energy efficiencies of the heating cogeneration and electrical power are plotted. Also, in figure 10 the exergy efficiencies of these parameters whit ORC are indicated. The amount of these values are reported in the 4.2.1 section. It can be seen that efficiencies have the very few changes to the temperature rise.

In figure 11, the mass flow rate of the Therminol-66 in different solar radiation modes based on the PTSC outlet temperature are shown. Its variations are between 480 to 620 K. In the solar mode the mass flow rate changes from 30 to 11 kg/s. In the solar and storage mode, it varies from 51 kg/s in the highest state to 24 kg/s in the lowest state. Finally, in the storage mode, this parameter is changed between 22-13 kg/s. So, PTSC outlet temperature has more effect on the working fluid mass flow rate. However, it is very economically parameters. Because it has a direct relationship with the number of the PTSC.

### 4.2.5. Exergy destruction rate

The exergy destruction rate and its percentage for the cycle are shown in figure 12. The baseline values that considered in this study are 365 K for the pump inlet temperature, and 2000 kPa for the turbine inlet pressure. Figure 12A illustrates the exergy destruction rate for each component in the

solar mode. The amount of the exergy destruction rate of the PTSC, ORC turbine, ORC pump, evaporator-b, heating process 1, and heating process 2 are 3520 kW (56%), 247.7 kW (4%), 9.5 kW (0.1%), 2063.1 kW (33%), 371.4 kW (6%), and 77.4 (0.9%), respectively. So, the PTSC and evaporator-b have the major exergy destruction rate in the solar mode.
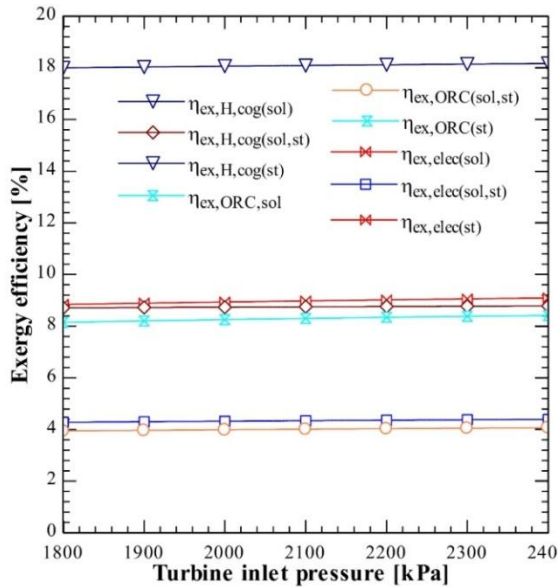


Figure 8. Effect of the turbine inlet pressure on the exergy efficiencies.

The solar and storage mode exergy destruction rate is shown in figure 12B. This value for the PTSC, ORC turbine, ORC pump, evaporator-b, heating process 1, heating process 2, storage heat exchanger, hot storage tank, and cold storage tank are 7230 kW (69%), 247.7 kW (2%), 9.5 kW (0.1), 2063.1 kW (20%), 371.4 kW (4%), 77.4 (0.9%),
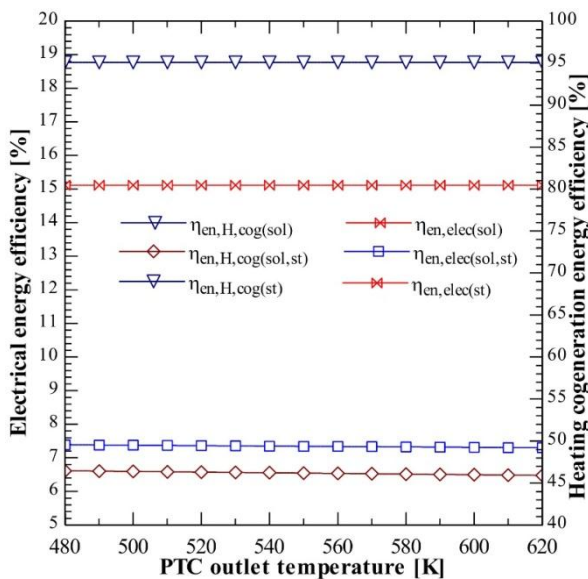


Figure 9. Effect of the PTSC outlet temperature on the energy efficiencies.
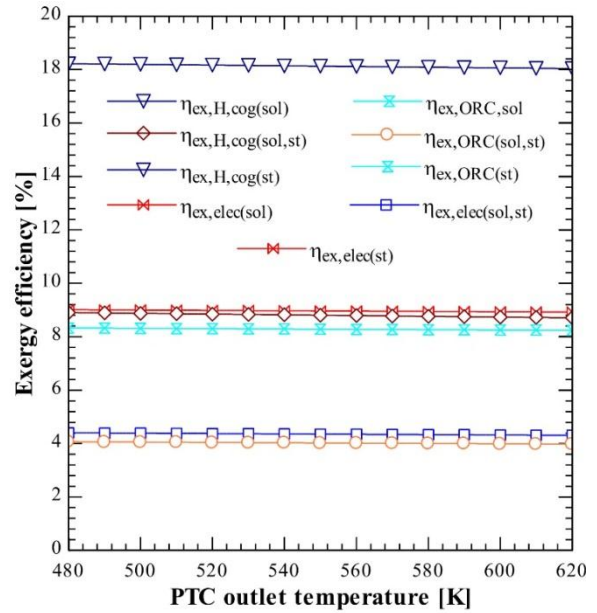


Figure 10. Effect of the PTSC outlet temperature on the exergy efficiencies.

120.4 (1%), 120.1 (1%), and 260.2 (2%), respectively.

Due to the increasing number of the PTSCs, their exergy destruction rate increased. Figure 12C is for the storage mode. In this mode, the PTSC does not exist. The exergy destruction rate for ORC turbine, ORC pump, evaporator-a, heating process 1, heating process 2, hot storage tank, and cold storage tank are 247.7 kW (14%), 9.5 kW (1), 729.4 kW (40%), 371.4 kW (20%), 77.4 kW (4%), 120.1 kW (7%), and 260.2 kW (14%), respectively. In this mode, the maximum exergy destruction rate is for evaporator-a.

## 5. Conclusions

Due to the archived results the following concluded can be written.

1. Monthly average daily absorbed solar radiation by the receiver of the PTSC during the year in Nazlou regain climate conditions are between 800-3700 W/m²/day. So, this regain as many different place in Iran has the high solar energy potential.

2. By using Therminol-66 as a working fluid for solar subsystem 470-660 K for PTSC outlet temperature and 53-56% efficiency for it are available during the year.

3. The total number of the PTSCs and their aperture to be responsive to energy demand at the engineering faculty of Urmia University are 500 and 35000 m² for solar mode and 250 and 17500 m² for the solar and storage mode, respectively.

4. Energy and exergy efficiencies in the solar mode and storage mode, are equal together. This equality occurs because, both storage tanks and PTSC are forced to supply the same energy.

5. Heating cogeneration and electrical power energy efficiencies in the solar mode and storage mode, are around 95% and 15%, respectively. Also, these parameters for the solar and storage mode, are around 45% and 7.5%, respectively. In addition, heating cogeneration, electrical power, and ORC exergy efficiencies for the solar mode and the storage mode, are around 18.5%, 9.5%, and 9% and for the solar and storage mode, are around 9%, 4.5%, and 4%, respectively.

6. The maximum exergy destruction rate in the solar mode, is for PTSC with 56%, in the solar and storage mode, is for PTSC with 68% and in the storage mode, is for ORC evaporator-a with 50%. Therefore, the PTSC and ORC evaporator have the major exergy destruction rate in the cycle.
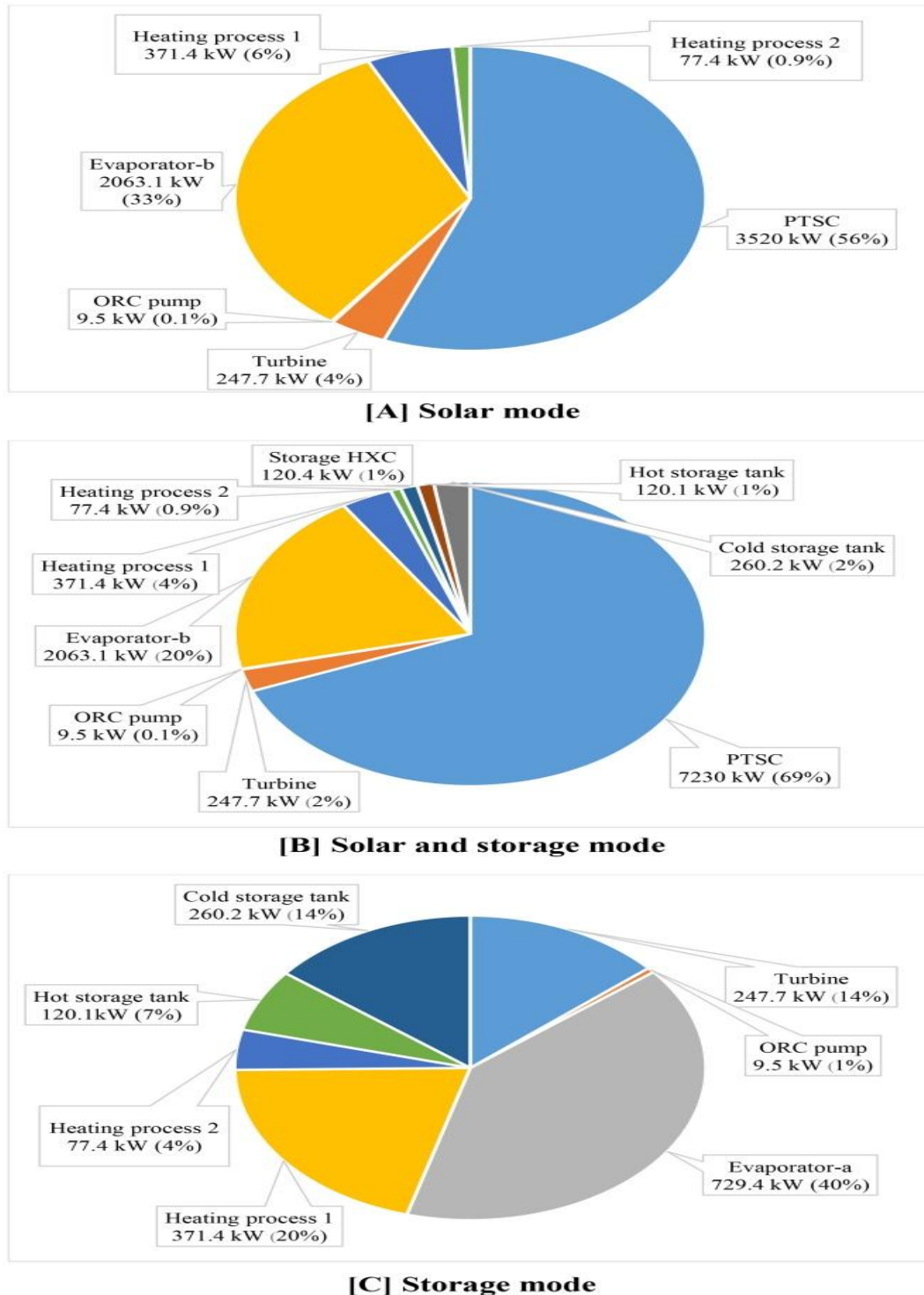


Figure 12. Exergy destruction rate of each component

**Nomenclature**

| | |
|---|---|
| A | area, $m^2$ |
| $C_p$ | specific heat, kJ/kg-K |
| D | diameter, m |
| EV | expansion valve |
| $\dot{EX}$ | exergy rate, kW |
| $F_R$ | heat removal factor |
| $F_1$ | collector efficiency factor |
| $G_b$ | monthly average daily beam radiation on a horizontal surface rate, $W/m^2$ |
| h | specific enthalpy, kJ/kg |
| $\bar{H}$ | radiation, $MJ/m^2$ |
| $\dot{I}$ | destruction exergy rate, kd |
| j | demand factor |
| k | thermal conductivity, W/m |
| $\bar{K}_t$ | clearness index |
| $\dot{m}$ | mass flow rate, kg/s |
| M | mass of the oil in the tank, kg |
| $N_{PTSC}$ | number of PTSC |
| NUS | Nusselt number |
| ORC | organic Rankine cycle |
| P | pressure, kPa |
| PTSC | parabolic trough solar collectors |
| Q | heat, kJ |
| $\dot{Q}$ | heat rate, kW |
| s | specific entropy, kJ/kg.K |
| $\bar{S}$ | monthly average daily radiation absorbed by receiver, $W/m^2$ |
| T | temperature, K |
| U | heat loss coefficient, $kW/m^2$ |
| w | collector width, m |
| $\dot{W}$ | power, kW |
| Z | solar azimuth angle, degree |

**Greek symbols**

| | |
|---|---|
| $\alpha$ | absorbance of the receiver, altitude angle, degree |
| $\delta$ | solar declination angle |
| $\varepsilon$ | emittance factor |
| $\omega$ | solar hour angle, degree |
| $\omega_s$ | hour angle at sunset or sunrise, degree |
| $\varphi$ | latitude angle (degree) |
| $\eta$ | efficiency, % |
| $\gamma$ | intercept factor |
| $\sigma$ | Stefane Boltzmann constant, $kW/m^2.K^4$ |
| $\rho$ | reflectance factor, density, $kg/m^3$ |
| $\tau$ | transmittance factor |

**Subscripts**

| | |
|---|---|
| 0 | atmospheric conditions |
| ap | aperture |
| c | cover |
| cog | cogeneration |
| cst | cold storage tank |
| d | diffuse |
| e | exit |
| en | energy |
| ev | evaporator |
| ex | exergy |
| g | generator |
| hp | heating process |
| H | heating |
| h,c | hot water consumed |
| hst | hot storage tank |
| i | inlet |
| l | lost |
| m | motor |
| o | outlet, overall |
| oe | organic cycle evaporator |
| op | organic cycle pump |
| r | Receiver, radiation |
| Sol,p | pump of the solar system |
| st,p1 | first pump in the thermal storage system |
| st,p2 | econd pump in the thermal storage system |
| tot | total |
| wp | water pump |
| u | useful |

**References**

[1] Kizilkan, O., Kabul, A. and Dincer, I., 2016. Development and performance assessment of a parabolic trough solar collector-based integrated system for an ice-cream factory. Energy, 100, pp.167-176.

[2] H.E., 1998. Solar distillation: a promising alternative for water provision with free energy, simple technology and a clean environment. Desalination, 116(1), pp.45-56.

[3] Fadai, D., 2007. Utilization of renewable energy sources for power generation in Iran. Renewable and Sustainable Energy Reviews, 11(1), pp.173-181.

[4] Alamdari, P., Nematollahi, O. and Alemrajabi, A.A., 2013. Solar energy potentials in Iran: A review. Renewable and Sustainable Energy Reviews, 21, pp.778-788.

[5] Kalogirou, S.A., 2013. Solar energy engineering: processes and systems. Academic Press.

[6] Duffie, J.A. and Beckman, W.A., 2013. Solar engineering of thermal processes. John Wiley & Sons.

[7] Suman, S., Khan, M.K. and Pathak, M., 2015. Performance enhancement of solar collectors—A review. Renewable and Sustainable Energy Reviews, 49, pp.192-210.

[8] Hafez, A.Z., Attia, A.M., Eltwab, H.S., ElKousy, A.O., Afifi, A.A., AbdElhamid, A.G., AbdElqader, A.N., Fateen, S.K., El-Metwally, K.A., Soliman, A. and Ismail, I.M., 2018. Design analysis of solar parabolic trough thermal collectors. Renewable and Sustainable Energy Reviews, 82, pp.1215-1260.

[9] Jebasingh, V.K. and Herbert, G.J., 2016. A review of solar parabolic trough collector. Renewable and Sustainable Energy Reviews, 54, pp.1085-1091.

[10] Macedo-Valencia, J., Ramírez-Ávila, J., Acosta, R., Jaramillo, O.A. and Aguilar, J.O., 2014. Design, construction and evaluation of parabolic trough collector as demonstrative prototype. Energy procedia, 57, pp.989-998.

[11] Ghodbane, M. and Boumeddane, B., 2016. Numerical analysis of the energy behavior of a Parabolic Trough concentrator. Journal of Fundamental and Applied Sciences, 8(3), pp.671-691.

[12] Eisavi, B., Khalilarya, S. and Chitsaz, A., 2018. Thermodynamic analysis of a novel combined cooling, heating and power system driven by solar energy. Applied Thermal Engineering, 129, pp.1219-1229.

[13] Al-Sulaiman, F.A., Hamdullahpur, F. and Dincer, I., 2012. Performance assessment of a novel system using parabolic trough solar collectors for combined cooling, heating, and power production. Renewable Energy, 48, pp.161-172.

[14] Marefati, M., Mehrpooya, M. and Shafii, M.B., 2018. Optical and thermal analysis of a parabolic trough solar collector for production of thermal energy in different climates in Iran with comparison between the conventional nanofluids. Journal of Cleaner Production, 175, pp.294-313.

[15] World weather Study Site website page. www.weather.com, 2017

[16] Tabatabaee M. Calculation of building's installation. Roozbehan publisher in Iran; 2003. (In Parsian)

[17] Bakirci, Kadir. "General models for optimum tilt angles of solar panels: Turkey case study." Renewable and Sustainable Energy Reviews 16, no. 8 (2012): 6149-6159.

[18] Liu, Benjamin YH, and Richard C. Jordan. "The interrelationship and characteristic distribution of direct, diffuse and total solar radiation." Solar energy 4, no. 3 (1960): 1-19.

[19] Bellos, E. and Tzivanidis, C., 2017. A detailed exergetic analysis of parabolic trough collectors. Energy Conversion and Management, 149, pp.275-292.

[20] Moran, M.J., Shapiro, H.N., Boettner, D.D. and Bailey, M.B., 2010. Fundamentals of engineering thermodynamics. John Wiley & Sons.

[21] Sonntag, R.E., Borgnakke, C., Van Wylen, G.J. and Van Wyk, S., 1998. Fundamentals of thermodynamics (Vol. 6). New York: Wiley.